3D Deployment of Multiple UAV-Mounted Base Stations for UAV Communications

Chen Zhang, Leyi Zhang, Lipeng Zhu, *Graduate Student Member, IEEE*, Tao Zhang, *Member, IEEE*, Zhenyu Xiao, *Senior Member, IEEE*, and Xiang-Gen Xia, *Fellow, IEEE*

***Abstract*— Recently, unmanned aerial vehicles (UAVs) have attracted lots of attention because of their high mobility and low cost. This article investigates a communication system assisted by multiple UAV-mounted base stations (BSs), aiming to minimize the number of required UAVs and to improve the coverage rate by optimizing the three-dimensional (3D) positions of UAVs, user clustering, and frequency band allocation. Compared with the existing works, the constraints of the required quality of service (QoS) and the service ability of each UAV are considered, which makes the problem more challenging. A three-step method is developed to solve the formulated mixed-integer programming problem. First, to ensure that each UAV can serve more number of users, the maximum service radius of UAVs is derived according to the required minimum power of the received signals for the users. Second, an algorithm based on artificial bee colony (ABC) algorithm is proposed to minimize the number of required UAVs. Third, the 3D position and the frequency band of each UAV are designed to increase the power of the target signals and to reduce the interference. Finally, simulation results are presented to demonstrate the superiority of the proposed solution for UAV-assisted communication systems.**

***Index Terms*— Wireless communication, unmanned aerial vehicles (UAVs), quality of service (QoS), base stations (BSs), three dimensional (3D) deployment.**

I. Introduction

THE fifth-generation (5G) mobile communication network targets for lager capacity, higher robustness, lower latency, and larger dense of users [1]. Nowadays, the number of mobile users and devices in the internet of things (IoT) is explosively increasing. It is forecasted that the number of IoT devices will reach 80 billion in the whole world by 2030 [2]. However, current terrestrial networks are facing great challenges to satisfy the access requirement. Especially for the remote areas lacking of terrestrial infrastructures and the disaster-affected areas with terrestrial infrastructures damaged, the communication service of ground users and devices cannot be satisfactorily guaranteed. Therefore, there is an urgent need for a new paradigm to improve the coverage ability of cellular networks.

Recently, unmanned aerial vehicle (UAV) has begun to play a more and more important role in assisting wireless communication networks and attract increasing attention, due to its high agility, high mobility, and high robustness of line-of-sight (LoS) channel [1], [3]–[9]. For an area having limited terrestrial infrastructures or facing an explosion of data traffic, UAVs can be employed as base stations (BSs) to offload the transmission tasks. Compared to ground BSs, UAVs can be used in many extreme environments and complex geographic conditions. Besides, thanks to their flexible and controllable mobility, UAVs can be rapidly deployed to the target areas and achieve on-demand coverage. Thus, UAV-assisted wireless communication is a promising technology for 5G or future wireless networks.

A. Related Works

In general, there are several typical topics about the application of UAVs as BSs, for example, the deploying of a single UAV or multiple UAVs [10]–[13], improving of the quality of service (QoS) [14]–[16], modeling of air to ground (A2G) channel [10], [17], planning of UAV's trajectory [18]–[22], cooperating of BSs and terrestrial infrastructures [23], [24], optimizing of energy efficiency [25], [26], and joint deployment and beamforming for UAV BS communication [27]–[29]. Among all these topics, the deployment of UAVs is a significant and fundamental one. Many researchers have contributed greatly to solving the problem of UAV deployment.

There are early works exploring the deployment of a single UAV. The authors in [10] modeled the A2G path loss for low altitude platforms (LAP), such as, BSs whose altitudes are less than 3000 meters. Their model showed that there are two main propagation groups, which are the LoS links and none-line-of-sight (NLOS) links via reflection and/or diffraction. In [11], the optimal altitude which can maximize the coverage region was obtained. In [30], a new three-dimensional (3D) deployment method of one UAV was proposed for maximum coverage under the constraint of users' different QoS. In [31], a method was proposed to obtain the 3D position of one UAV to cover the largest number of users in a certain area. In [32],

Manuscript received July 29, 2020; revised November 10, 2020; accepted December 27, 2020. Date of publication January 5, 2021; date of current version April 16, 2021. This work was supported in part by the National Key Research and Development Program under grant number 2020YFB1806800, the National Natural Science Foundation of China (NSFC) under grant numbers 61827901 and 91738301. The associate editor coordinating the review of this article and approving it for publication was R. Zhang. *(Corresponding authors: Tao Zhang; Zhenyu Xiao.)*

Chen Zhang, Leyi Zhang, Lipeng Zhu, Tao Zhang, and Zhenyu Xiao are with the School of Electronic and Information Engineering, Beihang University, Beijing 100191, China (e-mail: zhtao@buaa.edu.cn; xiaozy@buaa.edu.cn).

Xiang-Gen Xia is with the Department of Electrical and Computer Engineering, University of Delaware, Newark, DE 19716 USA.

Color versions of one or more figures in this article are available at https://doi.org/10.1109/TCOMM.2021.3049387.

Digital Object Identifier 10.1109/TCOMM.2021.3049387

TABLE I
MAIN CONTRIBUTION OF RELATED WORKS

Scenario	Reference	One sentence describing the main contribution	SINR Thresh-old	Service Ability	3D De-ploy-ment
Single UAV	Al-Hourani [10]	Modelling the A2G path loss for LAP.	No	No	Yes
	Al-Hourani [11]	Deriving the optimal altitude to maximize the coverage region.	No	No	No
	Yaliniz [31]	Optimizing the 3D position of one UAV to cover the largest number of users in a certain area.	No	No	Yes
	Chen [32]	Optimizing the 2D position of one UAV for a maximum number of users served by the UAV.	No	No	No
	Alzenad [33]	Maximizing the number of users served by one UAV as well as minimizing the transmit power.	Yes	No	Yes
Multi UAVs	Mozaffari [34]	Maximizing the coverage area and coverage lifetime of UAVs.	No	No	Yes
	Mozaffari [35]	Minimizing the transmit power of UAVs.	No	No	No
	Lyu [36]	Minimizing the number of UAVs needed to serve all the users.	No	No	No
	Zhao [39]	Deploying multi UAVs with known and unknown user locations while considering the maximum number of users served by each UAV.	Yes	Yes	No
	X. Liu [13]	Optimizing the deployment and movement of multiple UAVs to maximize the QoE.	Yes	No	Yes
	C. H. Liu [40]	Maximizing the fairness of the coverage of UAV.	No	No	No
	Qin [41]	Minimizing the number of required UAVs while considering service ability of each UAV.	No	Yes	Yes
	This Paper	Minimizing the number of required UAVs and improving the QoS of each user.	Yes	Yes	Yes

an improved multi-population genetic algorithm was proposed to optimize the 2D position of one UAV for a maximum number of users served by the UAV. In [33], a deployment method of UAV BS was proposed to maximize the number of served users as well as minimize the transmit power.

Nevertheless, as the distribution of users becomes more complicated and the demands for communication quality of users increase rapidly, it may be too difficult for a single UAV to assist the communication system. Therefore, lots of attention has been paid to the deployment problem of multiple UAVs. First, some works are devoted to deploy multiple UAVs according to the geographical situation. In [34], the 3D positions of UAVs were optimized to maximize the coverage area and coverage lifetime of UAVs. In [35], the optimal altitudes of UAVs were analyzed to obtain a certain coverage area that requires a minimum transmit power of UAVs. Then, to reduce the cost and ensure a full coverage of ground users, the authors in [36] proposed an ordered algorithm to minimize the number of UAVs required to serve all the ground users. Similarly, in [37] the elephant herding optimization algorithm [38] was utilized to minimize the number of required UAVs. In [39], the deployment problems of multiple UAVs with known and unknown user locations were studied, considering the constraint on the maximum number of users served by each UAV.

To further improve QoS, the research has been extended from 2D deployment to 3D deployment. In [13], a genetic algorithm based K-means (GAK-means) was applied to cluster users and the Q-learning algorithm was utilized to obtain the optimal deployment and movement of multiple UAVs, so as to maximize the quality of experience (QoE) of the UAV-assisted wireless network, but the number of UAVs is not optimized. Also using reinforcement learning method, an energy efficient approach was proposed in [40] to control UAVs to cover users in a fair way, while ignoring the coverage of a few users. In [41], the authors minimized the number of required UAVs by optimizing the positions of the UAVs using the edge-prior placement (EPP) algorithm, but the QoS of each user is not guaranteed. The scenarios and contributions of existing literatures for the deployment of UAV-assisted wireless networks are summarized in Table I.

B. Motivation and Contributions

Different from the existing works [11], [13], [34]–[36], [41], in this article, we consider to deploy multiple UAV BSs to serve ground users, where the coverage rate is maximized with as few as possible UAVs. In particular, we optimize the 3D positions of UAVs, user clustering, and frequency band allocation, under the constraints of service ability of each UAV and minimum signal-to-interference-plus-noise ratio (SINR) requirement of each user. The main contributions of this article are summarized as follows.

1) We formulate a 3D deployment problem incorporating both the service ability of UAVs and the QoS requirement of each user, which is shown to be a mixed-integer programming problem with NP-hard complexity. To solve this problem, we propose a sub-optimal solution with three steps, namely, maximum service radius determination, user clustering, and 3D deployment.
2) In the first step, to maximize the number of users covered by each UAV and to ensure the fairness of the

number of users served by each UAV, we derive the maximum service radius by theoretically controlling the altitudes of the UAVs. We particularly consider the altitude constraint of the UAVs and the QoS requirement of the users. The optimal altitude and the corresponding service radius are obtained by using the Karush-Kuhn-Tucker (KKT) conditions.

3) In the second step, given the maximum service radius, we minimize the number of user clusters, where each cluster is served by one UAV and the service ability, i.e., the maximum number of users that each UAV can serve, is taken into account. To solve this problem, we propose an ordered artificial bee colony (ABC)-based user clustering algorithm.
4) In the third step, given the user clustering, we optimize the 3D positions and band allocation for UAVs. Different from that in the first step where the altitudes of UAVs are optimized without attaching to specific users, the design in this step is to improve the QoS of the users by adjusting the 3D positions and optimizing the band allocation for UAVs, subject to a specific user clustering. In particular, the 2D position of each UAV is optimized to increase the received signal power. The frequency band of each UAV is optimized to decrease the inter-cluster interference. After that, the altitude of each UAV is optimized to minimize the maximum interference power of each user.
5) Finally, we evaluate the performance of the proposed algorithm for UAV-assisted wireless network. Simulation results show that compared to the benchmark schemes, the proposed strategy can significantly reduce the number of UAVs and improve the QoS.

C. Organization

The rest of this article is organized as follows. In Section II, we introduce the system model and formulate the problem for UAV deployment. In Section III, we provide our solution for the formulated problem. In Section IV, the simulation results are provided to show the superiority of the proposed solution. Finally, in Section V, we conclude this article.

Notation: a, $\boldsymbol{a}$ and $\mathcal{A}$ denote a scalar, a vector, and a set, respectively. $\mathbb{R}^{M\times 1}$ denotes the M-dimensional space of real numbers. $|\mathcal{A}|$ represents the cardinality of set $\mathcal{A}$. For two sets $\mathcal{A}_1$ and $\mathcal{A}_2$, $\mathcal{A}_2 \leftarrow \mathcal{A}_1$ denotes the insertion of all the elements of $\mathcal{A}_1$ into $\mathcal{A}_2$, while $\mathcal{A}_2 \subset \mathcal{A}_1$ means that $\mathcal{A}_2$ is a subset of $\mathcal{A}_1$, and $\mathcal{A}_2 \backslash \mathcal{A}_1$ represents the elements of $\mathcal{A}_2$ that are not included in $\mathcal{A}_1$. $\emptyset$ is an empty set.

II. System Model and Problem Formulation

As shown in Fig 1, we consider a downlink wireless communication system with multiple UAVs transmitting data to K ground users.[1] The users randomly distribute in a 2D rectangular area $\mathcal{D} = \{(x, y)|x_{min} \le x \le x_{max}, y_{min} \le y \le y_{max}\}$.

[1]Actually, the connectivity of the backbone network among UAVs should also be considered [39], [42]. In this article, we suppose the backbone network among UAVs and the access links between users and UAVs are with different frequencies. Furthermore, the bandwidth of the backbone links is assumed sufficiently large.

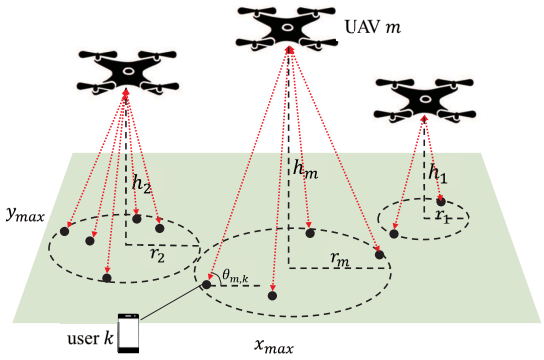

Fig. 1. The considered wireless communication system assisted by UAV BSs.

Let $\mathcal{K} = \{1, 2, \cdots, K\}$ denote the set of users. Each user $k \in \mathcal{K}$ has a fixed position $\boldsymbol{w}_k = [x_k, y_k]^{\mathrm{T}} \in \mathbb{R}^{2\times 1}$. Meanwhile, UAVs should be deployed in a 3D area $\mathcal{P} = \{(x, y, h)|x_{min} \le x \le x_{max}, y_{min} \le y \le y_{max}, h_{min} \le h \le h_{max}\}$, and we have $x_{min} < x_{max}$, $y_{min} < y_{max}$, and $h_{min} < h_{max}$. Let $\mathcal{M} = \{1, 2, \cdots, M\}$ denote the set of UAVs. The position of each UAV $m \in \mathcal{M}$ is $\boldsymbol{p}_m = [x_m, y_m, h_m]^{\mathrm{T}} \in \mathbb{R}^{3\times 1}$. Besides, let $\mathcal{B} = \{1, 2, , \cdots, B\}$ denote the set of available frequency bands and there is no interference between any two different frequency bands. Each UAV can utilize at most one frequency band to serve multiple users. The frequency band of UAV m is denoted by b_m, and the set of UAVs operating in band b is denoted by $\mathcal{M}_b$. For each cluster of users served by one UAV, orthogonal multiple access (OMA), such as orthogonal frequency division multiple access (OFDMA) and time division multiple access (TDMA), is employed. Thus, the intra-cluster interference is avoided. Due to the resource limitation for UAV platforms, we suppose that there are N_{max} orthogonal resource blocks in each frequency band, such as sub-carriers for OFDMA systems and time slots for TDMA systems. In each cluster, one resource block can only be used by one user for communication. Therefore, the service ability,[2] which means the maximum number of users that each UAV can serve, can be determined by N_{max}.

A. Channel Model

In the Internet-of-Things (IoT) and wireless communications, the channel model is a very important factor [43]–[45]. For wireless communications, the link between UAVs and users may be blocked by obstacles, such as, buildings and plants, causing a mixture of LoS and NLoS environments. Then, the large-scale coefficient of the channel between UAV m and user k is modeled by [46]:

$$\beta_{m,k}(d_{m,k}) = \begin{cases} \beta_0\, d_{m,k}^{-\alpha} & \text{LoS environment,} \\ \kappa\, \beta_0\, d_{m,k}^{-\alpha} & \text{NLoS environment,} \end{cases} \quad (1)$$

[2]In general, the service ability is determined by the available resource of a UAV and the requirement of users. For example, in [41], the service ability is defined as the capacity of a UAV divided by the average bandwidth requirement of each ground user. For TDMA systems, the service ability of a UAV may be given by the total number of time slots.

where β_0 is the path loss at the reference distance ($d_0 = 1\ m$) for LoS environments, $\kappa \in (0,1)$ is a real number which represents the attenuation loss for NLoS environments, α is the modeling parameter related to the path loss, $d_{m,k}$ is the distance between UAV m and user k, which can be represented as follow:

$$d_{m,k} = \sqrt{{h_m}^2 + {s_{m,k}}^2} = \frac{s_{m,k}}{\cos\theta_{m,k}}, \tag{2}$$

where h_m is the altitude of UAV and $s_{m,k}$ is the projected 2D distance between UAV m and user k which can be expressed as $s_{m,k} = \sqrt{(x_k - x_m)^2 + (y_k - y_m)^2}$, and $\theta_{m,k}$ is the elevation angle between UAV m and user k.

The probability of existing an LoS link between UAV m and user k is modeled by [46]:

$$P_{LoS}(\theta_{m,k}) = \frac{1}{1 + a\,\exp(-b(\theta_{m,k} - a))}, \tag{3}$$

where a and b are modeling parameters related to the environment. Then, we can obtain the probability of NLoS environment as $P_{NLoS}(\theta_{m,k}) = 1 - P_{LoS}(\theta_{m,k})$.

Thus, the channel gain between UAV m and user k can be modeled as follows [46]:

$$\begin{aligned}\bar{g}_{m,k}(d_{m,k},\theta_{m,k}) \triangleq\ & P_{LoS}(\theta_{m,k})\beta_0 {d_{m,k}}^{-\alpha} \\ & + P_{NLoS}(\theta_{m,k})\kappa\beta_0 {d_{m,k}}^{-\alpha} \\ =\ & \hat{P}_{LoS}(\theta_{m,k})\beta_0 {d_{m,k}}^{-\alpha},\end{aligned} \tag{4}$$

where $\hat{P}_{LoS}(\theta_{m,k}) = P_{LoS}(\theta_{m,k}) + P_{NLoS}(\theta_{m,k})\kappa$ represents a regularized LoS possibility [46], including both the LoS and NLoS environments.

We refer to the SINR of each user as the measurement of the communication quality. For user k, the SINR is given by:

$$E_{m,k} = \frac{P_{m,k}}{I_k + \sigma^2}, \tag{5}$$

where $P_{m,k}$ is the signal power received at user k from UAV m, I_k is the interference power at user k, and σ^2 is the power of the additive white Gaussian noise. $P_{m,k}$ and I_k can be calculated by equation (6) and equation (7), respectively.

$$P_{m,k} = \bar{g}_{m,k} \times P_t, \tag{6}$$

$$I_k = \sum_{m' \in \mathcal{M}_b \setminus m} P_{m',k}, \tag{7}$$

where P_t denotes the power of the transmit signal for each user and b is the band utilized by UAV m. In the considered system, we assume that the power of the transmit signal for each user is the same. Thus, the maximum transmit power for each UAV is upper-bounded by $N_{max}P_t$. Only when inequality $E_{m,k} \geq E_0$ is satisfied can user k successfully communicate with UAV m, where E_0 is the threshold of the SINR. We define an indicator function to represent the connection between users and UAVs, i.e.,

$$\gamma_{m,k} = \begin{cases} 1, & \text{user } k \text{ is served by UAV } m, \\ 0, & \text{otherwise}, \end{cases} \tag{8}$$

which means that user k is served by UAV m for $\gamma_{m,k} = 1$, and $\gamma_{m,k} = 0$ otherwise. Then, we define the coverage rate C as the percentage of the users being successfully served, which can be calculated by:

$$C = \frac{\sum_{m \in \mathcal{M}} \sum_{k \in \mathcal{K}} \gamma_{m,k}}{K}. \tag{9}$$

B. Problem Formulation

We aim to use the minimum number of UAVs to serve as many users as possible. However, with the increase of the coverage rate, more UAVs are required to be deployed. There is a basic tradeoff between the number of UAVs and the coverage rate. Therefore, we formulate the objective function as a weighted summation of the number of UAVs and the reciprocal of the coverage rate. The positions of UAVs, the connection between UAVs and ground users, and the frequency band allocation variables are jointly optimized as follows:

$$\min_{\{\boldsymbol{p}_m\},\{\gamma_{m,k}\},\{\mathcal{M}_b\}} \ \rho_1 |\mathcal{M}| + \frac{\rho_2}{C} \tag{10}$$

$$\text{s.t. } \boldsymbol{p}_m \in \mathcal{P}, \quad \forall m \in \mathcal{M}, \tag{10a}$$

$$\gamma_{m,k} \in \{0,1\}, \quad \forall k \in \mathcal{K}, \forall m \in \mathcal{M}, \tag{10b}$$

$$\sum_{m \in \mathcal{M}} \gamma_{m,k} \leq 1, \quad \forall k \in \mathcal{K}, \tag{10c}$$

$$\sum_{k \in \mathcal{K}} \gamma_{m,k} \leq N_{max}, \quad \forall m \in \mathcal{M}, \tag{10d}$$

$$\bigcup_{b \in \mathcal{B}} \mathcal{M}_b = \mathcal{M}, \tag{10e}$$

$$\mathcal{M}_b \bigcap \mathcal{M}_q = \emptyset, \quad \forall b, q \in \mathcal{B}, b \neq q, \tag{10f}$$

$$E_{m,k} \geq E_0 \gamma_{m,k}, \quad \forall k \in \mathcal{K}, \forall m \in \mathcal{M}, \tag{10g}$$

where ρ_1 and ρ_2 are the weight coefficients and $\rho_1 \ll \rho_2$ indicates that increasing the coverage rate has a priority over decreasing the number of UAVs. Constraint (10a) confines the feasible region of UAVs' position. Constraint (10b) specifies the range of $\gamma_{m,k}$. Constraint (10c) indicates that each user should be served by at most one UAV. Constraint (10d) indicates that the number of users served by each UAV should be no more than N_{max}. Constraints (10e) and (10f) indicate that each UAV should utilize one frequency band only. Constraint (10g) indicates the SINR requirement, i.e., QoS, for communication between UAV m and user k.

It is noteworthy that there are continuous variables and integer variables in the formulated problem, which is a mixed-integer programming problem with NP-hard complexity [47]. In the next section, we will develop a suboptimal solution of Problem (10).

III. Solution of the Problem

In this section, we propose a solution to solve the problem. First, since the coverage rate has a priority, we assume that all the users are successfully served by the UAVs, and minimize the number of UAVs. To this end, we optimize the altitudes of UAVs to derive the maximum service radius under the target power of received signals to make the number of users served by each UAV as close to N_{max} as possible, which can also ensure the fairness between different UAVs. Then, given the

maximum service radius, we propose an efficient algorithm to minimize the number of clusters of users, i.e., the number of UAVs. Finally, for each UAV serving one cluster, we optimize the 2D position of each UAV to maximize the minimum received power and allocate the band for each UAV to meet the SINR requirement of each user. After that, we optimize the altitudes of UAVs to reduce the maximum interference power of users.

A. Maximum Service Radius

Since the SINR of each user is highly coupled with the positions of UAVs, it is difficult to directly obtain the optimal solution of $\{\boldsymbol{p}_m\}$, $\{\gamma_{m,k}\}$, and $\{\mathcal{M}_b\}$. To simplify the original problem, we suppose only when $P_{m,k} \geq P_0$ can user k communicate with UAV m, where P_0 is defined as the minimum required power.[3] Define $\bar{g}_0 = \frac{P_0}{P_t}$ as the minimum channel gain for successful communication. Then, the constraint on $P_{m,k}$ can be transferred to a constraint on $\bar{g}_{m,k}$, i.e., $\bar{g}_{m,k} \geq \bar{g}_0$.

We define the maximum service radius as the largest 2D distance between a UAV and a user that enables communication. According to (4), the maximum service radius r_{ser} can be obtained by optimizing the flight altitude of the UAV. When there is no constraint for the altitude of UAV, the optimal altitude h_{opt} for the maximization of the maximum service radius has been obtained in [11]. However, when there exist constraints on the minimum and maximum altitudes, the solution in [11] may not always be feasible. In the following, we develop a solution for the maximization of the service radius.

We use h and r to denote the altitude and the service radius of one UAV, respectively. Then, the problem of maximizing the service radius can be formulated as follows:

$$\max_{r,h} \ r \tag{11}$$

$$\text{s.t.} \ \frac{1+\kappa a e^{-b(\arctan\frac{h}{r}-a)}}{1+a e^{-b(\arctan\frac{h}{r}-a)}}\beta_0 (r^2+h^2)^{-\frac{\alpha}{2}} \geq \bar{g}_0 \tag{11a}$$

$$h_{min} \leq h \leq h_{max}. \tag{11b}$$

Problem (11) can be solved according to KKT conditions.[4] We denote the elevation angle from a UAV to a ground user as θ. By using the trigonometric relation $h = r\tan\theta$, the problem can be described as follows:

$$\min_{r,\theta} \ -r \tag{12}$$

$$\text{s.t.} \ \bar{g}_0 - \frac{1+\kappa a e^{-b(\theta-a)}}{1+a e^{-b(\theta-a)}}\beta_0 \left(\frac{r}{\cos\theta}\right)^{-\alpha} \leq 0 \tag{12a}$$

$$r\tan\theta - h_{max} \leq 0 \tag{12b}$$

$$h_{min} - r\tan\theta \leq 0, \tag{12c}$$

[3]An upper bound on the interference power will be derived accordingly to satisfy the SINR constraint in Section III-C. An appropriate threshold P_0 should be selected to achieve the tradeoff between the signal power and interference power.

[4]Problem (11) is a non-convex problem, and thus the KKT conditions obtain a suboptimal solution.

and the Lagrange function is presented below:

$$\begin{aligned} L(r,\theta,\lambda_1,\lambda_2,\lambda_3) = &-r \\ &+\lambda_1[\bar{g}_0 - \frac{1+\kappa a e^{-b(\theta-a)}}{1+a e^{-b(\theta-a)}}\beta_0\left(\frac{r}{\cos\theta}\right)^{-\alpha}] \\ &+\lambda_2(r\tan\theta - h_{max}) + \lambda_3(h_{min} - r\tan\theta), \end{aligned} \tag{13}$$

where $\lambda_1, \lambda_2, \lambda_3$ indicate the Lagrange multipliers.

We use r_{ser} to represent the maximum service radius and θ^*, λ_1^*, λ_2^*, λ_3^* are the optimal solutions of the Lagrange duality problem which minimize the Lagrange function in (11). The following intermediate variables are adopted to simplify the function expressions:

$$\bar{g}^* = \frac{1+\kappa a e^{-b(\theta^*-a)}}{1+a e^{-b(\theta^*-a)}}\beta_0 (\frac{r_{ser}}{\cos\theta^*})^{-\alpha}, \tag{14}$$

$$\bar{g}_1' = \frac{\beta_0(\frac{r_{ser}}{\cos\theta^*})^{-\alpha}}{[1+a\,e^{\Theta}]^2}, \tag{15}$$

$$\bar{g}_2' = \frac{180}{\pi}(1-\kappa)abe^{\Theta} - \alpha\,\tan\theta^*(1+\kappa a e^{\Theta})(1+ae^{\Theta}), \tag{16}$$

$$\Theta = [-b(\frac{180}{\pi}\theta^* - a)]. \tag{17}$$

where $\bar{g}^*$ represents the optimal channel gain derived by substituting r_{ser} and θ^* into (4), $\bar{g}_1'$, $\bar{g}_2'$ and Θ are intermediate variables used to simplify expressions.

Therefore, according to the KKT conditions, the parameters should satisfy the following conditions:

$$\bar{g}_0 - \bar{g}^* \leq 0, \tag{18a}$$

$$r_{ser}\tan\theta^* - h_{max} \leq 0, \tag{18b}$$

$$h_{min} - r_{ser}\tan\theta^* \leq 0, \tag{18c}$$

$$\lambda_1^* \geq 0, \lambda_2^* \geq 0, \lambda_3^* \geq 0, \tag{18d}$$

$$\lambda_1^*(\bar{g}_0 - \bar{g}^*) = 0, \tag{18e}$$

$$\lambda_2^*(r_{ser}\tan\theta^* - h_{max}) = 0, \tag{18f}$$

$$\lambda_3^*(h_{min} - r_{ser}\tan\theta^*) = 0, \tag{18g}$$

$$\begin{aligned} \frac{\partial L}{\partial r} = -1 + \frac{\lambda_1^*\alpha}{\cos\theta^*}\frac{1+\kappa a e^{\Theta}}{1+ae^{\Theta}}(\frac{r_{ser}}{\cos\theta^*})^{-\alpha-1} \\ +\lambda_2^*\tan\theta^* - \lambda_3^*\tan\theta^* = 0, \end{aligned} \tag{18h}$$

$$\frac{\partial L}{\partial \theta} = -\lambda_1^*\bar{g}_1'\bar{g}_2' + \frac{\lambda_2^* r_{ser}}{\cos^2\theta^*} - \frac{\lambda_3^* r_{ser}}{\cos^2\theta^*} = 0, \tag{18i}$$

Based on the above analysis, a general form of r_{ser} and the optimal θ^* can be derived according to the following three propositions.

Proposition 1: If $\lambda_2^* = \lambda_3^* = 0$, then r_{ser} is given by:

$$r_{ser} = \frac{\cos\theta^*}{\log_\alpha(\frac{g_0}{\bar{P}_{LoS}(\theta^*)})\beta_0}. \tag{19}$$

Proof: If $\lambda_2^* = \lambda_3^* = 0$, then $h_{min} < r_{ser}\tan\theta^* < h_{max}$ according to (18f) and (18g). Therefore, (18h) and (18i) can be rewritten as:

$$\frac{\partial L}{\partial r} = -1 + \frac{\lambda_1^*\alpha}{\cos\theta^*}\frac{1+\kappa a e^{\Theta}}{1+ae^{\Theta}}(\frac{r_{ser}}{\cos\theta^*})^{-\alpha-1} = 0, \tag{20}$$

$$\frac{\partial L}{\partial \theta} = -\lambda_1^*\bar{g}_1'\bar{g}_2' = 0. \tag{21}$$

Based on (20), λ_1^* can be presented as:

$$\lambda_1^* = \frac{1}{\frac{\alpha}{\cos\theta^*}\frac{1+\kappa a e^{\Theta}}{1+ae^{\Theta}}(\frac{r_{ser}}{\cos\theta^*})^{-\alpha-1}}, \tag{22}$$

which is a positive value. Hence, according to (18e), the following equation must be satisfied:

$$\bar{g}_0 - \bar{g}^* = 0. \tag{23}$$

Since $\lambda_1^* > 0$ and $\bar{g}_1' > 0$, (21) can be simplified as $\bar{g}_2' = 0$, where θ^* is the only unknown variable and can be obtained by using the bisection search. By inserting θ^* into (23), the optimal service radius r_{ser} is given by (19). ■

Proposition 2: If $\lambda_2^* > 0$, $\lambda_3^* = 0$, then r_{ser} is given by:

$$r_{ser} = \frac{\cos\theta^*}{\log_{\alpha+1}\frac{(1-\lambda_2^*\tan\theta^*)\cos\theta^*(1+ae^{\Theta})}{\lambda_1^*\alpha(1+\kappa a e^{\Theta})}}. \tag{24}$$

Proof: If $\lambda_2^* > 0$, $\lambda_3^* = 0$, we have $r_{ser}\tan\theta^* = h_{max}$ according to (18f) and (18g). Therefore, (18h) and (18i) can be rewritten as:

$$\frac{\partial L}{\partial r} = -1 + \frac{\lambda_1^*\alpha}{\cos\theta^*}\frac{1+\kappa a e^{\Theta}}{1+ae^{\Theta}}(\frac{r_{ser}}{\cos\theta^*})^{-\alpha-1} + \lambda_2^*\tan\theta^* = 0, \tag{25}$$

$$\frac{\partial L}{\partial \theta} = -\lambda_1^*\bar{g}_1'\bar{g}_2' + \frac{\lambda_2^* r_{ser}}{\cos^2\theta^*} = 0. \tag{26}$$

Based on (26), λ_1^* can be presented as:

$$\lambda_1^* = \frac{\lambda_2^* r_{ser}}{\cos^2\theta^*\bar{g}_1'\bar{g}_2'}, \tag{27}$$

which is a positive value according to (18d). Thus, (23) should also be satisfied as well.

By solving simultaneous equations (23), (25), (26) and $r_{ser}\tan\theta^* = h_{max}$, $\theta^*, \lambda_1^*, \lambda_2^*$ can be determined, and r_{ser} is given by (24). ■

Proposition 3: If $\lambda_2^* = 0$, $\lambda_3^* > 0$, then r_{ser} is given by:

$$r_{ser} = \frac{\cos\theta^*}{\log_{\alpha+1}\frac{(1+\lambda_3^*\tan\theta^*)\cos\theta^*(1+ae^{\Theta})}{\lambda_1^*\alpha(1+\kappa a e^{\Theta})}}. \tag{28}$$

Proof: If $\lambda_2^* = 0$, $\lambda_3^* > 0$, we have $r_{ser}\tan\theta^* = h_{min}$ according to (18f) and (18g). Therefore, (18h) and (18i) can be rewritten as:

$$\frac{\partial L}{\partial r} = -1 + \frac{\lambda_1^*\alpha}{\cos\theta^*}\frac{1+\kappa a e^{\Theta}}{1+ae^{\Theta}}(\frac{r_{ser}}{\cos\theta^*})^{-\alpha-1} - \lambda_3^*\tan\theta^* = 0, \tag{29}$$

$$\frac{\partial L}{\partial \theta} = -\lambda_1^*\bar{g}_1'\bar{g}_2' - \frac{\lambda_3^* r_{ser}}{\cos^2\theta^*} = 0. \tag{30}$$

Based on (29), λ_1^* can be presented as:

$$\lambda_1^* = -\frac{\lambda_3^* r_{ser}}{\cos^2\theta^*\bar{g}_1'\bar{g}_2'}, \tag{31}$$

which is a positive value according to (18d). Thus, (23) should also be satisfied.

By solving simultaneous equations (23), (29), (30) and $r_{ser}\tan\theta^* = h_{min}$, $\theta^*, \lambda_1^*, \lambda_3^*$ can be determined, and r_{ser} is give by (28).

■

Considering the above three propositions, the maximum service radius r_{ser} is obtained as follows:

$$r_{ser} = \begin{cases} \dfrac{\cos\theta^*}{\log_{\alpha}(\frac{g_0}{\bar{P}_{LoS}(\theta^*)})\beta_0}, & \lambda_2^*=\lambda_3^*=0, \\ \dfrac{\cos\theta^*}{\log_{\alpha+1}\frac{(1-\lambda_2^*\tan\theta^*)\cos\theta^*(1+ae^{\Theta})}{\lambda_1^*\alpha(1+\kappa a e^{\Theta})}}, & \lambda_2^*>0,\ \lambda_3^*=0, \\ \dfrac{\cos\theta^*}{\log_{\alpha+1}\frac{(1+\lambda_3^*\tan\theta^*)\cos\theta^*(1+ae^{\Theta})}{\lambda_1^*\alpha(1+\kappa a e^{\Theta})}}, & \lambda_2^*=0,\ \lambda_3^*>0, \end{cases} \tag{32}$$

and the corresponding altitude of the UAV is given by $h^* = r_{ser}\tan\theta^*$. Note that if $\lambda_2 > 0$ and $\lambda_3 > 0$ hold simultaneously, we have $r_{ser}\tan\theta^* = h_{max}$ and $r_{ser}\tan\theta^* = h_{min}$ according to (18f) and (18g), respectively. It contradicts with the fact $h_{max} > h_{min}$. Thus, all possible solutions of problem (12) are derived in (32). The feasible region of the KKT equation (18) is divided to three subspaces, which correspond to the three cases of different values of λ_2^* and λ_3^* in (32). For each case, we should solve the corresponding equation set to obtain λ_2^* and λ_3^* and verify whether the obtained solutions satisfy the priori condition on λ_2^* and λ_3^* of this case. The obtained solutions that satisfy the priori condition are compared, and the one which achieves the maximum service radius is the final solution. From the above three propositions, we observe that the maximum service radius is influenced by both the altitude constraint and the minimum channel gain for successful communication. When $h_{min} \le h_{opt} \le h_{max}$ holds, which corresponds to case 1 in (32), the altitude of UAV for maximizing the service radius is given by h_{opt}. For $h_{opt} > h_{max}$ and $h_{opt} < h_{min}$ cases, which correspond to case 2 and case 3 in (32), the altitude of UAV for maximizing the service radius is given by h_{max} and h_{min}, respectively, because the optimal altitude does not satisfy the constraint. For all three cases, the maximum service radius is readily to be derived for the given altitude of UAV as shown in (32).

Deploying a UAV at proper altitude $h^* = r_{ser}\tan\theta^*$, a user who has $s_{m,k} = r_{ser}$ always satisfies $\bar{g}_{m,k} = \bar{g}_0$. Thus, we can transfer the constraint of channel gain, as shown in (10g), into the constraint of service radius, expressed as follows:

$$\gamma_{m,k}s_{m,k} \le r_{ser}, \tag{33}$$

which means the distance between UAV m and a user k served by it should be no more than r_{ser}.

And Problem (10) can be rewritten as follow:

$$\min_{\{\boldsymbol{p}_m\},\{\gamma_{m,k}\}} \quad |\mathcal{M}| \tag{34}$$

$$\text{s.t. } \boldsymbol{p}_m \in \mathcal{P}, \quad \forall m \in \mathcal{M}, \tag{34a}$$

$$\gamma_{m,k} \in \{0,1\}, \quad \forall k \in \mathcal{K}, \forall m \in \mathcal{M}, \tag{34b}$$

$$\sum_{m\in\mathcal{M}} \gamma_{m,k} = 1, \quad \forall k \in \mathcal{K}, \tag{34c}$$

$$\sum_{k\in\mathcal{K}} \gamma_{m,k} \le N_{max}, \quad \forall m \in \mathcal{M}, \tag{34d}$$

$$\gamma_{m,k}s_{m,k} \le r_{ser}, \quad \forall k \in \mathcal{K}, \forall m \in \mathcal{M}. \tag{34e}$$

Note that Problem (34) is also a mixed-integer programming problem, which is difficult to solve. Therefore, an *Ordered*

ABC-based Placement (OAP) algorithm is proposed to deal with the problem. The algorithm consists of two parts. First, we determine the service users of each UAV by clustering users into different groups, each group of users is served by one UAV. Then, we decide the 3D position of each UAV according to the clustering condition.

B. User Clustering

In this subsection, we propose an algorithm to cluster users into different groups. User clustering is helpful to solve problem in wireless communication [48]–[51]. Users in group m are served by UAV m, whose number should be no more than N_{max} considering the service ability of each UAV. The largest service area of each UAV is a circular area with the position of UAV as the center and r_{max} as the radius. The service users of each UAV must be within the largest service area of the UAV, and the number of service users should be as close as N_{max} in order to minimize the number of required UAVs.

Therefore, the user clustering problem is simplified as follow:

$$\min_{\{\gamma_{m,k}\}} \quad |\mathcal{M}| \tag{35}$$

$$\text{s.t. } \gamma_{m,k} \in \{0,1\}, \quad \forall k \in \mathcal{K}, \forall m \in \mathcal{M}, \tag{35a}$$

$$\sum_{m \in \mathcal{M}} \gamma_{m,k} = 1, \quad \forall k \in \mathcal{K}, \tag{35b}$$

$$\sum_{k \in \mathcal{K}} \gamma_{m,k} \leq N_{max}, \quad \forall m \in \mathcal{M}, \tag{35c}$$

$$\gamma_{m,k} r_{m,k} \leq r_{ser}, \quad \forall k \in \mathcal{K}, \forall m \in \mathcal{M}.. \tag{35d}$$

In order to solve this problem, we develop a hybrid algorithm combining heuristic algorithm and ABC algorithm, which is the first part of our OAP algorithm. The heuristic algorithm, referring to [36] and [41], can reduce the solution space of ABC algorithm so that the proper solution can be found more quickly. ABC algorithm is effective in finding the optimal solution under constraints [52].

In the m-th iteration, the goal is to determine the center position F_c^m of group m, ensuring the group to contain as many users as possible. First, we find users located at the boundary of uncovered area and put them into the set of boundary users $\mathcal{K}_{bo}$ while other users are in the set of inner users $\mathcal{K}_{in}$. Then, the boundary user farthest from the center of the uncovered area will be picked up as feature user k_0 of the group. The selection of k_0 can effectively reduce the existence of isolated users, who cannot be covered by one UAV with other users. Feature user k_0 is selected as shown in Fig. 2.

After selecting feature user, users at a distance of more than $2r_{ser}$ away from user k_0 are removed from consideration because they are impossible to be served by the same UAV with user k_0. Such process can reduce the invalid solution space of ABC algorithm. We define the set of users whose distance from k_0 does not exceed $2r_{ser}$ as $\mathcal{K}_{local}$ and divided them into the set of boundary users $\mathcal{K}_{local,bo}$ and the set of inner users $\mathcal{K}_{local,in}$. After that, the center of the cluster F_c^m is

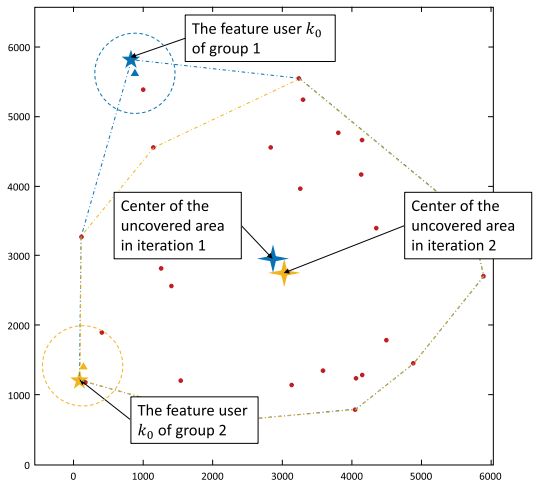

Fig. 2. The selection method of feature user k_0.

Algorithm 1: Ordered ABC-Based User Clustering Algorithm

Input:
User set $\mathcal{K}$, user locations $\{\boldsymbol{w}_k\}$
Output:
The number of groups $|\mathcal{M}|$ and set $\mathcal{L}$
1: Initialize $m = 1$, $\mathcal{L} = \emptyset$, $\mathcal{K}_U = \mathcal{K}$
2: **while** $\mathcal{K}_U \neq \emptyset$ **do**
3: Find boundary user set $\mathcal{K}_{U,bo} \subseteq \mathcal{K}_U$ and update inner user set $\mathcal{K}_{U,in} \leftarrow \mathcal{K}_U \backslash \mathcal{K}_{U,bo}$.
4: Choose $k_0 \in \mathcal{K}_{U,bo}$ which is farthest from the center of the uncovered area
5: Add every boundary user whose distance to k_0 is no more than $2r_{ser}$ to the set $\mathcal{K}_{local,bo}$.
Add every inner user whose distance to k_0 is no more than $2r_{ser}$ to the set $\mathcal{K}_{local,in}$.
6: Use Algorithm 2 to obtain $\mathcal{L}^m$.
7: Set $\mathcal{K}_U \leftarrow \mathcal{K}_U \backslash \mathcal{L}^m$.
8: Update $m = m + 1$.
9: Add $\mathcal{L}^m$ to $\mathcal{L}$.
10: **end while**
11: $|\mathcal{M}| = m$.
return $\mathcal{L}$, $|\mathcal{M}|$.

determined by applying ABC algorithm and a group of users $\mathcal{L}^m \subset \mathcal{K}$ is obtained as well.

For each user $l \in \mathcal{L}^m$, we have $\gamma_{m,l} = 1$, which means this group of users will be served by UAV m.

The above process repeats until all the users are grouped. Details of the proposed algorithm are provided in Algorithm 1.

Algorithm 1 describes the process of clustering users into different groups. Step 10 invokes ABC algorithm to decide the center of cluster, which is detailed in Algorithm 2.

ABC algorithm was proposed by Karaboga in 2005 to solve multivariable function optimization problems [52]. The idea behind the formulation is to find the proper solutions by imitating the behavior of employed bees, onlooker bees and scout bees cooperating with each other to search for food. The algorithm is described as follows.

Algorithm 2: ABC Procedure

Input: $\{w_k\}_{k\in\mathcal{K}} \in \mathbb{R}^{2\times 1}$, $\mathcal{K}_{local,bo}$, $\mathcal{K}_{local,in}$, k_0, N_{max}, r_{ser}, N_p, T_{abc}, T_s

Output: $\mathcal{L}^m$

Randomly initialize the set of possible positions for cluster's center $\mathcal{F}^{(0)}$, $t = 1$.
while $t \leq T_{abc}$ **do**
  if $t = 1$ **then**
    Calculate the fitness values of the positions in $\mathcal{F}^{(0)}$. Record the greatest fitness value f_c^m and the optimal position F_c^m.
  end if
  for $i = 1 : N_p$ **do**
    Pick a location $F_i^{(t)}$ in the neighborhood of $F_i^{(t-1)}$. Calculate the distance $s(F_i^{(t)},k_0)$, and normalize it if $s(F_i^{(t)}, k_0) > r_{ser}$.
    Calculate its fitness value $f_i^{(t)}$ and compare it with $f_i^{(t-1)}$. Choose the one with greater fitness value.
  end for
  For each $F_i^{(t)}$, calculate $P_i = \frac{0.9 * f_i^{(t)}}{\max\limits_i f_i^{(t)}} + 0.1$.
  for $j = 1 : |\mathcal{F}_0|$ **do**
    for $i = 1 : N_p$ **do**
      Generate a random number n.
      if $n < P_i$ **then**
        Break.
      end if
      if $i == N_p$ **then**
        $i = 1$
      end if
    end for
    Select a position $F_{i_{new}}^{(t)}$ in the neighborhood of $F_i^{(t)}$. Examine the distance $s(F_{i_{new}}^{(t)}, k_0)$ and normalize the distance if $s(F_{i_{new}}^{(t)}, k_0) > r_{ser}$.
    Calculate the fitness value of $F_{i_{new}}^{(t)}$ and replace $F_i^{(t)}$ with $F_{i_{new}}^{(t)}$ if it has a greater fitness value.
  end for
  Calculate the greatest fitness value $\max\limits_i f^{(t)}$ in $\mathcal{F}^{(t)}$ and updated f_c^m and F_c^m if $\max\limits_i f^{(t)} > f_c^m$.
  If no position around $F_i^{(t)}$ has larger fitness value than $F_i^{(t)}$ after T_s times iteration, randomly generate a new $F_i^{(t)}$.
  Update $t = t + 1$.
end while
Add users located in the circle with center F_c^m and radius r_{ser} to set $\mathcal{L}^m$.
return $\mathcal{L}^m$.

1) *Initialization*: We generate the initial solution set $\mathcal{F}^{(0)} = \{F_1^{(0)}, \cdots, F_{N_p}^{(0)}\}$, where N_p represents the total number of solutions. Every initial solution $F_i^{(0)} = (x_i^{(0)}, y_i^{(0)})$ is a possible position for the center of the current cluster and the distance between every position and k_0 is no more than r_{ser}.

2) *Fitness Value Calculation*: After initialization, we start searching for the best position of the cluster's center according to different bees' behavior. The iteration t is taken as an example to illustrate the iterative process.
For every solution $F_i^{(t)}$, we calculate its fitness values in order to find the optimal solution F_c^m with the highest fitness value f_c^m. The fitness value of $F_i^{(t)}$ is defined as:

$$f_i^{(t)}(x_i^{(t)}, y_i^{(t)}) = \begin{cases} \alpha_1 N_{bo} + \alpha_2 N_{in}, \\ \qquad N_{bo} + N_{in} \leq N_{max}. \\ 0.01, \quad N_{bo} + N_{in} > N_{max}. \end{cases} \tag{36}$$

where N_{bo} indicates the number of boundary users in $\mathcal{K}_{local,bo}$ covered by the circle with $F_i^{(t)}$ as center and r_{ser} as radius, while N_{in} indicates the number of inner users in $\mathcal{K}_{local,bo}$ covered by the circle. α_1 and α_2 represent the weights of N_{bo} and N_{in}, respectively, and satisfy $\alpha_1 > \alpha_2$. Users located on the boundary should be preferentially covered compared to inner users because the reduction of a boundary user may lead to a reduction for the number of UAVs [36]. The fitness value means when the number of users covered by the circle is no more than N_{max}, the more covered users, the more likely for $F_i^{(t)}$ to be chosen as the optimal solution. However, when the number of users covered by the circle is more than N_{max}, which means that the number of users exceeds the maximum service ability of UAV, we set a penalty factor $f_i^{(t)} = 0.01$ to avoid this situation.
By calculating the fitness values of all candidate positions, we obtain the maximum fitness value f_c^m and the best position F_c^m among those possible positions.

3) *Employed Bees Phase*: For $t > 1$, an employed bee searches for another possible position $F_i^{(t)}$ for cluster's center in its neighborhood as follows:

$$F_i^{(t)}(e) = F_i^{(t-1)}(e) + \phi(F_i^{(t-1)}(e) - F_j^{(t-1)}(e)), \tag{37}$$

where $e = 1, 2$ represents the x or y coordinate, $j \neq i$, and $\phi \in [-1, 1]$ is a random number. $F_i^{(t-1)}$ is the position of the employed bee in the $(t-1)$-th iteration. First, to calculate the 2D distance between feature user k_0 and every possible position $F_i^{(t)}$, we define $s(F_i^{(t)}, k_0) = \sqrt{(x_i^{(t)} - x_{k_0})^2 + (y_i^{(t)} - y_{k_0})^2}$ as the 2D distance function. If $s(F_i^{(t)}, k_0) > r_{ser}$, which means the cluster with center $F_i^{(t)}$ can not cover k_0, we select the new position $F_i^{\prime(t)} = (x_i^{\prime(t)}, y_i^{\prime(t)})$ to replace $F_i^{(t)}$ by normalizing $s(F_i^{(t)}, k_0)$ to be r_{ser}, which is given by

$$\begin{cases} x_i^{\prime(t)} = \dfrac{r_{ser}}{s(F_i^{(t)}, k_0)}(x_i^{(t)} - x_{k_0}) + x_{k_0}, \\ y_i^{\prime(t)} = \dfrac{r_{ser}}{s(F_i^{(t)}, k_0)}(y_i^{(t)} - y_{k_0}) + y_{k_0}. \end{cases} \tag{38}$$

After examining and adjusting the position of $F_i^{(t)}$, we calculate its fitness value $f_i^{(t)}$ and compare it with the fitness value of $F_i^{(t-1)}$. The one with higher fitness

value is selected as the new candidate position. Finally, the set of cluster centers $\mathcal{F}^{(t)}$ is derived.

4) *Onlooker Bees Phase*: Onlooker bees start searching in the neighborhood of the candidate positions according to a probabilistic model. For position $F_i^{(t)}$, the probability of being chosen by an onlooker bee is given by [52]:

$$P_i = \frac{0.9 * f_i^{(t)}}{\max\limits_i \ f_i^{(t)}} + 0.1, \tag{39}$$

where $\max\limits_i \ f_i^{(t)}$ presents the greatest fitness value of the positions in $\mathcal{F}^{(t)}$. Every onlooker bee generates a random real number $n \in (0,1)$. If $n < P_i$, then the onlooker bee chooses $F_i^{(t)}$ and search for a new position $F_{i_{new}}^{(t)}$ in its neighborhood according to (37). After adjusting the position and calculate its fitness value, the one with higher fitness value will replace $F_i^{(t)}$. Finally, the position set $\mathcal{F}^{(t)}$ is updated.

Then we recalculate the greatest fitness value $\max\limits_i \ f_i^{(t)}$ of the positions in $\mathcal{F}^{(t)}$ and compare it with f_c^m. If it is greater than f_c^m, then we update f_c^m and the optimal position F_c^m.

5) *Scout Bees Phase*: If no better position is found after searching T_s times, where T_s represents the largest searching time, the old position will be given up while the scout bee will randomly generate a new position and start its searching. It is an effective process to remove local optimums at the expense of computational complexity.

The iteration will be repeated until the iteration time is up to the maximum value T_{abc}. The position F_c^m with the maximum fitness value is selected as the final position for the cluster's center. The users located in the circle with center F_c^m and radius r_{ser} are stored in set $\mathcal{L}^m$.

When operating the proposed user clustering algorithm, Algorithm 2 is invoked to obtain the cluster center and the users assigned to each group. In Algorithm 2, the complexity of line 1 is $\mathcal{O}(N_p\,|\mathcal{K}_{local}|)$. For each iteration, the complexity of lines 2-26 is $\mathcal{O}(2N_p\,|\mathcal{K}_{local}|)$. After iteration, the complexity of line 27 is $\mathcal{O}(|\mathcal{K}_{local}|)$. Thus, the complexity of Algorithm 2 is $\mathcal{O}(T_{abc}N_p\,|\mathcal{K}_{local}|)$. Consequently, the computational complexity of the proposed algorithms for user clustering is $\mathcal{O}(T_{abc}N_p\,|\mathcal{M}|\,|\mathcal{K}_{local}|)$.

C. 3D Deployment and Band Allocation

For given $\mathcal{L} = \{\mathcal{L}^1, \cdots, \mathcal{L}^{|\mathcal{M}|}\}$, user $l \in \mathcal{L}^m$ satisfies $\gamma_{m,l} = 1$. For each group, one UAV should be deployed to serve the users. Note that the altitude optimization for the UAVs in Section III-A is to theoretically derive the maximum service radius. However, the SINRs of users within the service radius are not taken into account. Thus, the main idea of the proposed 3D deployment method is to improve the SINR. The 2D position of each UAV is optimized to improve the received signal power. The frequency bands are allocated to UAVs and the altitude of each UAV is adjusted to reduce the interference.

1) 2D Deployment: First, the 2D position of UAV m is optimized.[5] To maximize the channel gain between m and its service users in $\mathcal{L}^m$, the 2D distance between UAV m and users in $\mathcal{L}^m$ should be as short as possible. Therefore, we should minimize the 2D distance between UAV m and the farthest user in $\mathcal{L}^m$, which can be expressed as follow:

$$\min_{\{x_m, y_m\}} \ \max_{l \in \mathcal{L}^m} \ s_{m,l} \tag{40}$$

$$\text{s.t. } x_{min} \le x_m \le x_{max} \quad \forall m \in \mathcal{M}, \tag{40a}$$

$$y_{min} \le y_m \le y_{max} \quad \forall m \in \mathcal{M}, \tag{40b}$$

where $s_{m,l}$ denotes the 2D distance between UAV m and user l in $\mathcal{L}^m$.

The above problem is a convex optimization problem and can be solved by using optimization tools such as CVX [53]. Then, the 2D coordinates (x_m, y_m) of UAV m are obtained, and the smallest service radius r_{min}^m of UAV m to serve all the users in $\mathcal{L}^m$ is determined as:

$$r_{min}^m = \max_{l \in \mathcal{L}^m} \ s_{m,l}. \tag{41}$$

2) Band Allocation: After determining the 2D positions of all UAVs, we allocate the frequency bands. According to (5) and (7), since the received signal power of user k served by UAV m satisfies $P_{m,k} \ge P_0$, to meet the SINR constraint $E_{m,k} \ge E_0$, an upper bound on the interference at user k from UAV $m' \in \mathcal{M}_{b_m}$ is defined as follows:

$$P_{m',k} \le \frac{P_0/E_0 - \sigma^2}{|\mathcal{M}| - 1}. \tag{42}$$

The channel gain between user k and UAM m' is represented as $\bar{g}_{m',k} = \frac{P_{m',k}}{P_t}$, and constraint (42) is equivalent to

$$\bar{g}_{m',k} \le \frac{P_0/E_0 - \sigma^2}{(|\mathcal{M}| - 1) \times P_t} \triangleq \hat{g}_0. \tag{43}$$

Similar to the definition of the maximum service radius, the minimum interference radius is defined as the smallest 2D distance between UAV m' and user k that ensures the interference channel gain no larger than $\hat{g}_0$. Specifically, the interference radius r_{interf} can be derived by substituting the optimal altitude h^* into (43). If the 2D distances between user k served by UAV m and the other UAVs in the same band with UAV m are no smaller than the minimum interference radius, i.e., $s_{m',k} \ge r_{interf}$, $\forall m' \in \mathcal{M}_{b_m}$, the SINR constraint of user k is satisfied.

To reduce the inter-cluster interference, we develop the following band allocation algorithm, which tries to keep the distances between the UAVs in the same frequency band as large as possible. In line 1, $\mathcal{M}_U$ represents the set of UAVs which have not been allocated with frequency band. Then, $|\mathcal{B}|$ UAVs are allocated with orthogonal frequency bands and removed from $\mathcal{M}_U$ as shown in lines 2 and 3.

Subsequently, in lines 4-16, we allocate the frequency bands to the other UAVs in a successive manner. For each UAV $m_i \in \mathcal{M}_U$, we choose UAV $m_{b,close} \in \mathcal{M}_b$ which is the closest to

[5] In the user clustering phase, the channel gains of the users located within the service radius are not considered. Hence, we need to optimize the positions of UAVs and take the QoS of each user into account.

Algorithm 3: Band Allocation

Input: $\mathcal{M}$, $\mathcal{L}$, $\mathcal{B}$
Output: $\{\mathcal{M}_b|b \in \mathcal{B}\}$
1: Initialization: $\mathcal{M}_U = \mathcal{M}$, $\mathcal{M}_b = \emptyset, \forall b \in \mathcal{B}$.
2: Select the UAV m_1 closest to the center of the area. $\mathcal{M}_1 \leftarrow m_1$, $\mathcal{M}_U = \mathcal{M}_U \setminus m_1$.
3: Select $|\mathcal{B}|-1$ UAVs closest to UAV m_1, namely, UAV $m_2, \cdots, m_{|\mathcal{B}|}$. $\mathcal{M}_2 \leftarrow m_2, \cdots, \mathcal{M}_B \leftarrow m_{|\mathcal{B}|}$, $\mathcal{M}_U = \mathcal{M}_U \setminus \{m_2, \cdots, m_{|\mathcal{B}|}\}$.
4: **for** $i = |\mathcal{B}|+1 : |\mathcal{M}|$ **do**
5: Select the UAV $m_i \in \mathcal{M}_U$ closest to UAV m_1, $\mathcal{M}_{close} = \emptyset$
6: **for** $b = 1 : |\mathcal{B}|$ **do**
7: Select the UAV $m_{b,close} \in \mathcal{M}_b$ closest to UAV m_i, $\mathcal{M}_{close} \leftarrow m_{b,close}$, calculate $s(m_i, m_{b,close})$, $n(m_i, m_{b,close})$.
8: **end for**
9: Select UAV m_{b_1} and m_{b_2} from $\mathcal{M}_{close}$, where UAV m_{b_1} satisfies $s(m_i, m_{b_1}) = \max_{b \in \mathcal{B}} s(m, m_{b,close})$, UAV m_{b_2} satisfies $n(m_i, m_{b_2}) = \min_{b \in \mathcal{B}} n(m, m_{b,close})$. If UAV m_{b_2} is not unique, choose the one with higher $s(m_i, m_{b_2})$
10: **if** $n(m_i, m_{b_1}) = 0$ **then**
11: $\mathcal{M}_{b_1} \leftarrow m_i$.
12: **else**
13: $\mathcal{M}_{b_2} \leftarrow m_i$.
14: **end if**
15: $\mathcal{M}_U = \mathcal{M}_U \setminus m_i$, $m_1 = m_i$.
16: **end for**
return $\{\mathcal{M}_b|b \in \mathcal{B}\}$.

UAV m_i in each frequency band, and the set of the selected UAVs is given by $\mathcal{M}_{close} = \{m_{1,close}, \cdots, m_{B,close}\}$. Two measurements are defined as the 2D distance from UAV m_i to UAV $m_{b,close}$, $s(m_i, m_{b,close})$, and the number of UAV m_i's users that suffer interference exceeding $\hat{g}_0$ from UAV $m_{b,close}$, $n(m_i, m_{b,close})$. To reduce the interference, the distance between two UAVs in the same frequency bands should be as large as possible, and the number of users which suffer interference lager than $\hat{g}_0$ should be as small as possible. Thus, in line 9, we select two candidate bands b_1 and b_2 which can achieve the maximum $s(m_i, m_{b,close})$ and the minimum $n(m_i, m_{b,close})$, respectively. If $n(m_i, m_{b_1}) = 0$, which means that the users served by UAV m_i all satisfy constraint (43) in band b_1, then band b_1 is allocated to UAV m_i. Otherwise, band b_2 is allocated to UAV m_i to guarantee the number of users which do not satisfy constraint (43) as small as possible.

3) Altitude Adjustment: Since both the service and interference radiuses change with the flight altitude, we optimize the altitudes of UAVs to improve the SINRs of users.

Let $\mathcal{L}^c$ represents users served by other UAVs in band b. We first calculate the smallest 2D distance s_{min} between UAV m and users in $\mathcal{L}^c$. which is presented as:

$$s_{min} = \min_{l \in \mathcal{L}^c} s_{m,l}. \tag{44}$$

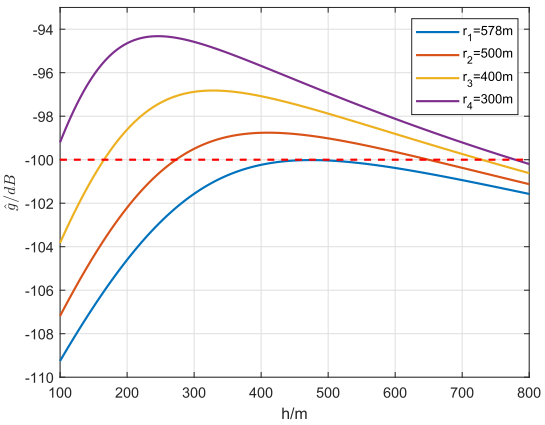

Fig. 3. Curve of channel gain $\hat{g}_0$ as a function of h_m when r_m is fixed.

Then, the altitude of UAV m is adjusted as follow:

1) If $s_{min} > r_{interf}$
The interference power of each user served by other UAVs from UAV m satisfies (42), the altitude h_m is adjusted to improve the received signal power of users served by UAV m. According to (4), channel gain reduces with increasing distance between the UAV and user. Thus, in order to improve the QoS of the served users, we maximize the channel gain between UAV m and the user which is served by and the farthest from UAV m, and the 2D distance of them is given by r^m_{min}. Then the altitude h_m is calculated as:

$$h_m = \begin{cases} h_{min}, & r^m_{min} \tan\theta^* < h_{min}, \\ r^m_{min} \tan\theta^*, & h_{min} \le r^m_{min} \tan\theta^* \le h_{max}, \\ h_{max}, & r^m_{min} \tan\theta^* > h_{max}, \end{cases} \tag{45}$$

where θ^* is the optimal θ in Proposition 1.

2) If $r^m_{min} < s_{min} < r_{interf}$
To reduce the interference, the interference radius r_{interf} of UAV m should be adjusted as follows:

$$r_{interf} = s_{min} - \varepsilon, \tag{46}$$

where ε is a small positive number. Since the channel gain $\bar{g}_{m,l}$ satisfies $\bar{g}_{m,l} = \hat{g}_0$ when $s_{m,l} = r_{interf}$, ε guarantees $s_{min} > r_{interf}$, ensuring the interference power from UAV m to user l satisfies constraint (42). To satisfy the constraint on interference power of user l from UAV m, the altitude h_m should satisfy:

$$\bar{g}(r_{interf}, h_m) = \hat{g}_0, \tag{47}$$

and to ensure UAV m can serve users in $\mathcal{L}^m$, the altitude h_m should satisfy:

$$\bar{g}(r^m_{min}, h_m) = \bar{g}_0. \tag{48}$$

According to Fig. 3, we can obtain $h_{m_1,l}$ and $h_{m_1,s}$ from (47), where $h_{m_1,s} \le h_{m_1,l}$. Besides, $h_{m_2,l}$ and $h_{m_2,s}$, $h_{m_2,s} \le h_{m_2,l}$ can also be obtained from (48). The designed altitude is given by $h_m = \max\{h_{m_1,s}, h_{m_2,s}, h_{min}\}$.

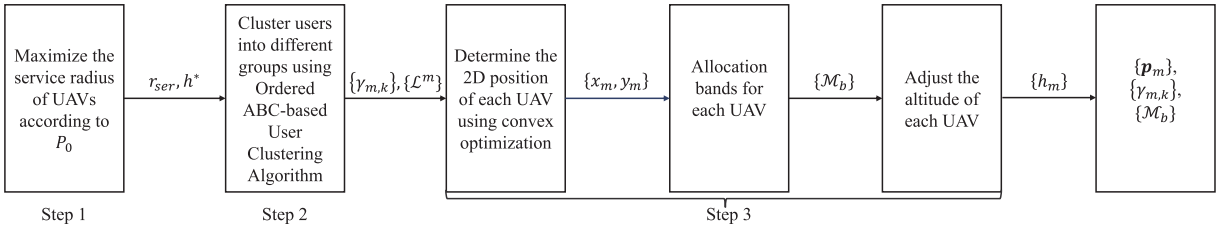

Fig. 4. The flowchart of overall solution for joint UAV deployment, user assignment, and frequency band allocation.

3) If $s_{min} < r^m_{min}$
Since r^m_{min} is the smallest service radius of UAV m, if $s_{m,l} = s_{min}$, the SINR of user l cannot be ensured by adjusting the service radius. After excluding user l from $\mathcal{L}^c$, we can obtain $\mathcal{L}'^c = \mathcal{L}^c \backslash l$, where each user $l \in \mathcal{L}'^c$ satisfies $s_{m,l} > r^m_{min}$. Then the smallest 2D distance s'_{min} between UAV m and users in $\mathcal{L}'^c$ is derived, which satisfies $r^m_{min} < s'_{min} < r_{interf}$.
Therefore, the interference radius r_{interf}, the optimal altitude h_m, and the service radius r_m of UAV m are derived according to (46), (47) and (48), respectively.

However, for different parameter settings, the solution of equation (47) may be different. As shown in Fig.3, the channel gain $\bar{g}_(r_{interf}, h_m)$ changes with h_m under different fixed r_{interf}. It is observed that in some cases, there are two solutions for equation (47). We use $h_{m,s}$ and $h_{m,l}$ to represent the two solutions and suppose $h_{m,s} < h_{m,l}$. If $h_{m,s} < h_{min}$, h_{min} should be chosen as the altitude of the UAV m. If $h_{min} < h_{m,s} < h_{max}$, $h_{m,s}$ should be chosen as the altitude of the UAV m.

Hereto, we obtain a suboptimal solution of the joint UAV deployment, user clustering, and frequency band allocation problem for multi-UAV assisted wireless communication systems. The overall scheme of the proposed solution is shown in Fig. 4. The computational complexity of user clustering is $\mathcal{O}(T_{abc}N_p\,|\mathcal{M}|\,|\mathcal{K}_{local}|)$ as discussed in Section III-B. The complexity of determining UAVs' 2D position is $\mathcal{O}(|\mathcal{M}|\,N_{max})$. The complexity of band allocation is $\mathcal{O}(|\mathcal{M}|^2)$, and the complexity of altitude adjusting is $\mathcal{O}(|\mathcal{M}|)$. Therefore, the computational complexity of the overall algorithm is $\mathcal{O}(|\mathcal{M}|^2 + T_{abc}N_p\,|\mathcal{K}_{local}|\,|\mathcal{M}|)$.

IV. Performance Simulations

In this section, we provide and analyze the simulation results. In our simulations, the communication system considered is composed of ground users and UAVs. The minimum altitude of UAVs is $h_{min} = 100$m, while the maximum altitude of UAVs is $h_{max} = 500$m.[6] We consider a sophisticated urban environment [54], where $a = 11.95$, $b = 0.14$ and $\alpha = 2$. Therefore, we can calculate $\theta^* = 0.69$, $r_{ser} = 578m$, respectively. Other parameter constraints in the simulation process are shown in Table II.

[6]The proposed algorithms can be applied for any altitude range and it only provides a theoretical guidance for UAV deployment. According to the system setting, the optimal altitude of UAV for maximizing the coverage radius is $h^* = 477$m. Thus, we choose this altitude range for simulation similar to a few other existing literatures, such as $200 \sim 500$m in [54] and $0 \sim 600$m in [55], even though it may need political approval [56].

TABLE II
Simulation Parameters

Parameter	Physical Meaning	Value
x_{min}, y_{min}	Lower bound of the feasible region	0 m
β_0	Path loss parameter	7×10^{-5} [46]
κ	Attenuation loss parameter	0.01 [46]
T_{abc}	Maximum iteration times of ABC algorithm	800
T_s	Largest searching time of scout bees	100
N_p	Population size of ABC algorithm	500
N_{max}	Service ability	8
ε	Small positive number	1
E_0	Threshold of SINR	2
σ^2	Variance of AWDN	-110 dBm [54]
P_t	Transmit signal power	30 dBW
$\bar{g}_0$	Threshold of channel gain	-100 dB

We choose K-means-based placement (KMP) algorithm, ordered PSO-based placement (OPP) algorithm, unordered ABC-based placement (UAP) algorithm and Edge-Prior Placement (EPP) algorithm [41] as benchmark schemes in the simulation.

KMP algorithm uses K-means clustering algorithm to cluster users. Obviously, in the scenario where the number of users is $|\mathcal{K}|$ and the service ability of each UAV is N_{max}, the minimum number of required UAVs is $|\mathcal{K}|\,/N_{max}$. Therefore, we start from using $|\mathcal{K}|\,/N_{max}$ UAVs and check whether the constraints of UAV's service radius and service ability are satisfied. If not, add one UAV and repeat the above step until all clusters meet the constraints.

OPP algorithm applies the same heuristic algorithm as OAP algorithm when finding k_0, but uses PSO algorithm instead of ABC algorithm to cluster users. The maximum iteration times and the population sizes of PSO algorithm are the same as those of ABC algorithm.

UAP algorithm uses ABC algorithm directly without combining with heuristic algorithm. Unlike OAP algorithm, UAP algorithm picks a k_0 randomly without distinguishing whether it is a boundary point or inner point.

EPP is the algorithm proposed in [41]. In each iteration, the boundary user farthest from the center of the uncovered area is selected as k_0. The $N_{max} - 1$ users the closest to k_0 are selected to evaluate whether the smallest circle covering these N_{max} users meet the constraint of UAV's service radius.

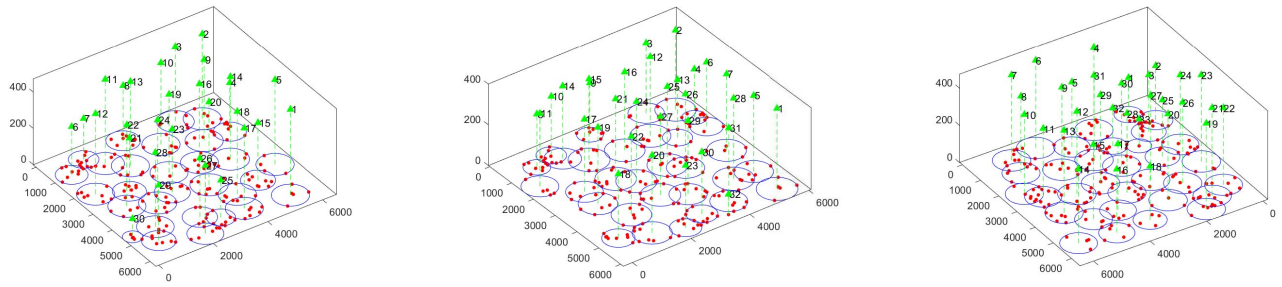

(a) Total number of UAVs using OAP algorithm:30 (b) Total number of UAVs using EPP algorithm:32 (c) Total number of UAVs using OPP algorithm:33

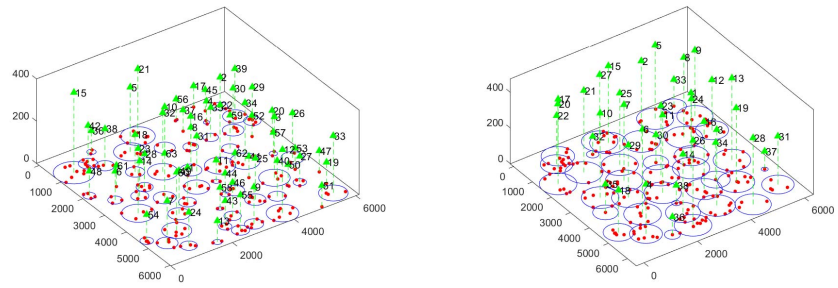

(d) Total number of UAVs using KMP algorithm:63 (e) Total number of UAVs using OAP algorithm:38

Fig. 5. Deployment conditions of the same user distribution using different algorithms.

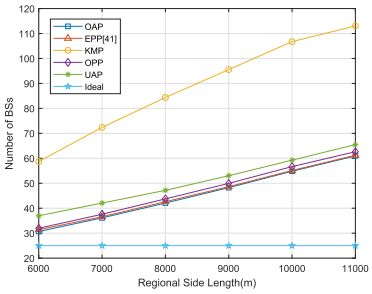

(a) Comparison of required number of UAVs with varying regional area when using different algorithms, where the service ability is 8 and the number of users is 200.

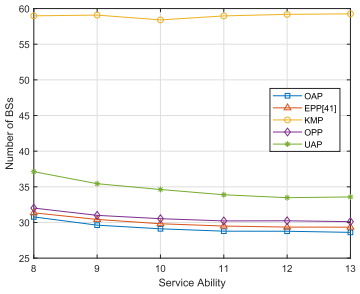

(b) Comparison of required number of UAVs with varying service ability when using different algorithms, where the regional side length is 6000m and the number of users is 200.

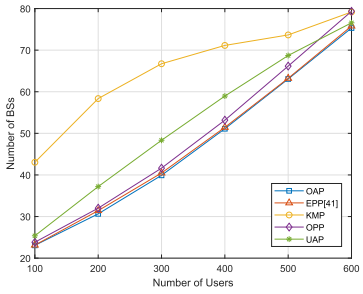

(c) Comparison of required number of UAVs with varying number of users when using different algorithms, where the regional side length is 6000m and the service ability is 8.

Fig. 6. Comparison of number of required UAVs when using different algorithms.

If not, reduce one user from the selected $N_{max}-1$ users and continue to find the smallest circle covering the other users until the radius meets the constraint.

A. The Performance of Reducing the Number of UAVs

The grouping results of users obtained by OAP algorithm, EPP algorithm, OPP algorithm, KMP algorithm and UAP algorithm are shown in Fig. 5, where 200 users are randomly distributed in 6km×6km area and the service ability of each UAV is 8. The simulation results show that all of these 5 algorithms can solve the grouping problem of users while satisfying the constraints, while OAP algorithm has a better performance on reducing the number of UAVs.

Fig. 6 presents the result of comparing the number of required UAVs with varying conditions when using different algorithms. Each point is an average result of 100 different distributions. It can be observed that compared with the benchmark schemes, the proposed algorithm significantly performs the best in minimizing the number of UAVs. In particular, KMP scheme requires the largest number of UAVs. Since OPP uses the same heuristic algorithm as OAP, the result reveals that using the proposed heuristic algorithm can effectively reduce the number of UAVs. While the number of UAVs obtained by OAP is less than OPP, which shows the superiority of ABC algorithm compared with PSO algorithm. For EPP scheme, when deploying each UAV, it requires to exhaustively search the combinations of $N_{max}-1$ users until the service radius constraint is satisfied. Thus, the computational complexity of the deployment of each UAV is $\mathcal{O}(2^{N_{max}-1})$. Compared with EPP, the proposed solution significantly reduces the computational complexity to a polynomial time.

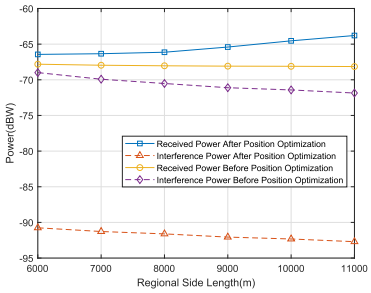

(a) Comparison of received power and interference power with varying regional area before and after optimization, where the service ability is 8, the number of bands is 8, and the number of users is 200.

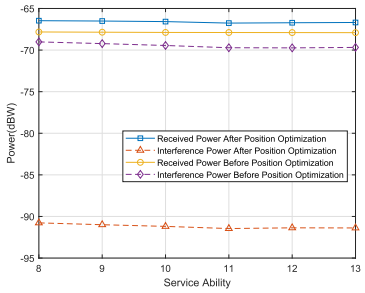

(b) Comparison of received power and interference power with varying service ability before and after optimization, where the regional side length is 6000m, the number of bands is 8, and the number of users is 200.

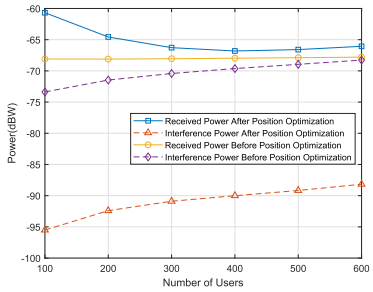

(c) Comparison of received power and interference power with varying number of users before and after optimization, where the regional side length is 10000m, the number of bands is 8, and the service ability is 8.

Fig. 7. Comparison of received power and interference power before and after optimization.

Fig. 6(a) shows the comparison of UAVs' number with varying distribution regional area. It can be observed that with enlarging regional area, more UAVs are needed to cover all the users because the user distribution is less dense, making it more and more difficult to cover many users by one UAV considering the constraint on UAV's service radius, and the phenomenon is similar for all schemes. Besides, the ideal solution is obtained based on the assumption that the service radius of UAVs is infinite, which means that the number of UAV BSs is given by $|\mathcal{K}|/N_{max}$. It can be noticed that when the regional side length is relatively small, the proposed solution is close to the lower-bound provided by the ideal solution. However, with the regional side length increasing, the gap between the proposed solution and the ideal solution becomes more and more obvious.

The number of required UAVs with varying service ability is shown in Fig. 6(b). When the service ability of UAVs is relatively small, we can see a similar phenomenon for the four schemes that the number of required UAVs decreases with increasing service ability. However, with growing service ability, the service radius limits the number of users that one UAV can actually serve. In this case, other benchmark schemes can not find the optimal solution, while OAP algorithm performs the best in reducing the number of UAVs.

In Fig. 6(c), it is observed that the number of UAVs increases when the number of users increases. That is because the constraint on service ability limits the number of users one UAV can serve. Thus, more number of UAVs have to be deployed to the region in order to serve the increasing number of users.

The simulation results show that no matter how the environment or the service ability changes, OAP algorithm can always find the solution with the smallest number of UAVs in a polynomial level of computational complexity, verifying the superiority of the proposed user clustering algorithm.

B. The Performance of Improving Communication Quality

The effectiveness of improving the QoS by optimizing the position and communication band of each UAV can be evaluated by examining the average interference power and the average received power of all users. The comparison of interference power and received power with varying condition for $P_t = 30$ dBW is shown in Fig. 7. Each point is an average result of 100 different distributions.

Fig. 7(a) shows the comparison of received power and interference power before and after the optimization of 3D positions and band allocation with varying distribution regional area. It is observed that the received power increases and the interference power decreases when the region enlarges. The reason is that for a larger region, the distribution of users becomes less dense, making it less possible for a UAV to cover users served by other UAVs and offer better service for its users. Fig. 7(b) shows the comparison of received power and interference power before and after the optimization of 3D positions and band allocation with varying service ability of UAVs. We can see that the received power does not change much while the interference power decreases with increasing area. That is because with increasing service ability, more users located in a UAV's service region can be served by the UAV. Therefore, fewer users act as interference. In Fig. 7(c), the received power decreases and the interference power increases as the number of users increases. The increasing number of users results in the distribution of users to be more dense, which increases the number of UAVs in the same band and thus introduces more interference.

However, when examining the three figures in Fig. 7 together, we can find that no matter how the environment or the service ability of UAV changes, the received power after optimization always increases, and the interference power decreases obviously after optimization, indicating the effectiveness of optimizing UAV's positions in improving communication quality.

Fig. 8(a) shows the coverage rate with varying distribution regional areas. It can be observed that the coverage rate increases when the region enlarges. Since the increasing area leads to the distribution of users to be less dense, the interference power of each user decreases and thus the coverage rate is enhanced. Fig. 8(b) shows the coverage rate with varying service abilities of UAVs. It can be observed that the coverage rate increases with the increasing of service ability. The reason is as follows. As the service ability of each UAV

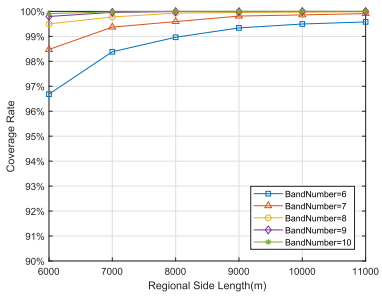

(a) Comparison of coverage rate with varying regional area under different number of bands, where the service ability is 8 and the number of users is 400.

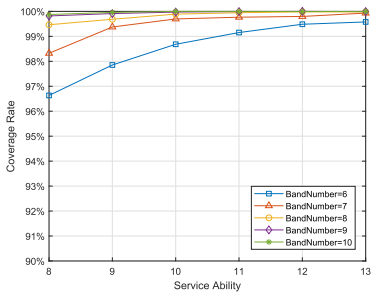

(b) Comparison of coverage rate with varying service ability under different number of bands, where the regional side length is 6000m and the number of users is 400.

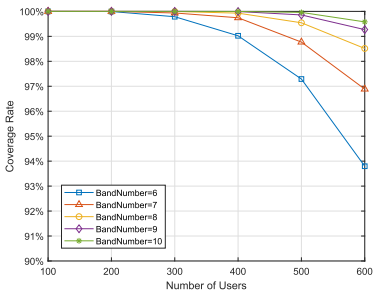

(c) Comparison of coverage rate with varying number of users under different number of bands, where the regional side length is 8000m and the service ability is 8.

Fig. 8. Comparison of coverage rate with different simulation parameters.

increases, the number of required UAVs decreases, and thus the inter-cluster interference reduces. In Fig. 8(c), it can be observed that the coverage rate decreases with the increasing number of users. This is because when the number of users increases, users are more and more likely to be located in the interference area of other UAVs.

For all scenarios, we can find that the coverage rate is always close to 100%, which indicates the superiority of the proposed solution in maximizing the coverage rate of users. Besides, the coverage rate increases with the increasing number of frequency bands. This is because more available frequency bands can reduce the number of UAVs in the same frequency band and thus reduce the interference.

In summary, for the UAV 3D deployment problem under constraint on service ability studied in this article, OAP algorithm proposed in this article can effectively reduce the number of UAVs, and the optimization of UAVs' 3D positions and frequency bands can reduce the system interference and increase the channel gain to improve the communication quality of the system.

V. Conclusion

In this article, we proposed a solution for deploying multiple UAVs as BSs to serve ground users, considering the QoS requirement of the users and the service ability of the UAVs. The UAV deployment, user clustering, and band allocation were optimized to minimize the number of required UAVs and improve the coverage rate of the users. The solution was divided into three steps. First, the maximum service radius of UAVs satisfying the power requirement was derived theoretically by applying KKT conditions. Second, an order ABC-based algorithm was proposed to solve the problem of minimizing the number of required UAVs under the constraints of the service radius and service ability. Third, we allocated the frequency band for UAVs and optimized their 3D positions to improve the QoS of the users given a specific user clustering. In the last section, the simulation results were presented. Compared to benchmark schemes, the proposed solution can achieve a superior performance in terms of minimizing the number of UAVs and improving the coverage rate of users.

References

[1] B. Li, Z. Fei, and Y. Zhang, "UAV communications for 5G and beyond: Recent advances and future trends," *IEEE Internet Things J.*, vol. 6, no. 2, pp. 2241–2263, Apr. 2019.

[2] L. Chettri and R. Bera, "A comprehensive survey on Internet of Things (IoT) toward 5G wireless systems," *IEEE Internet Things J.*, vol. 7, no. 1, pp. 16–32, Jan. 2020.

[3] K. P. Valavanis and G. J. Vachtsevanos, *Handbook of Unmanned Aerial Vehicles*. Dordrecht, The Netherlands: Springer, 2015.

[4] Y. Zeng, R. Zhang, and T. J. Lim, "Wireless communications with unmanned aerial vehicles: Opportunities and challenges," *IEEE Commun. Mag.*, vol. 54, no. 5, pp. 36–42, May 2016.

[5] Z. Xiao, P. Xia, and X.-G. Xia, "Enabling UAV cellular with millimeter-wave communication: Potentials and approaches," *IEEE Commun. Mag.*, vol. 54, no. 5, pp. 66–73, May 2016.

[6] S. Sekander, H. Tabassum, and E. Hossain, "Multi-tier drone architecture for 5G/B5G cellular networks: Challenges, trends, and prospects," *IEEE Commun. Mag.*, vol. 56, no. 3, pp. 96–103, Mar. 2018.

[7] D. Liu *et al.*, "Opportunistic utilization of dynamic multi-UAV in device-to-device communication networks," *IEEE Trans. Cognit. Commun. Netw.*, vol. 6, no. 3, pp. 1069–1083, Sep. 2020.

[8] L. Zhu, J. Zhang, Z. Xiao, X. Cao, X.-G. Xia, and R. Schober, "Millimeter-wave full-duplex UAV relay: Joint positioning, beamforming, and power control," *IEEE J. Sel. Areas Commun.*, vol. 38, no. 9, pp. 2057–2073, Sep. 2020.

[9] Z. Ullah, F. Al-Turjman, and L. Mostarda, "Cognition in UAV-aided 5G and beyond communications: A survey," *IEEE Trans. Cognit. Commun. Netw.*, vol. 6, no. 3, pp. 872–891, Sep. 2020.

[10] A. Al-Hourani, S. Kandeepan, and A. Jamalipour, "Modeling air-to-ground path loss for low altitude platforms in urban environments," in *Proc. IEEE Global Commun. Conf.*, Dec. 2014, pp. 2898–2904.

[11] A. Al-Hourani, S. Kandeepan, and S. Lardner, "Optimal LAP altitude for maximum coverage," *IEEE Wireless Commun. Lett.*, vol. 3, no. 6, pp. 569–572, Dec. 2014.

[12] L. Liu, S. Zhang, and R. Zhang, "CoMP in the sky: UAV placement and movement optimization for multi-user communications," *IEEE Trans. Commun.*, vol. 67, no. 8, pp. 5645–5658, Aug. 2019.

[13] X. Liu, Y. Liu, and Y. Chen, "Reinforcement learning in multiple-UAV networks: Deployment and movement design," *IEEE Trans. Veh. Technol.*, vol. 68, no. 8, pp. 8036–8049, Aug. 2019.

[14] B. Van Der Bergh, A. Chiumento, and S. Pollin, "LTE in the sky: Trading off propagation benefits with interference costs for aerial nodes," *IEEE Commun. Mag.*, vol. 54, no. 5, pp. 44–50, May 2016.

[15] H. Li and X. Zhao, "Throughput maximization with energy harvesting in UAV-assisted cognitive mobile relay networks," *IEEE Trans. Cognit. Commun. Netw.*, early access, Apr. 17, 2020, doi: 10.1109/TCCN.2020.2988556.

[16] A. M. Almasoud and A. E. Kamal, "Data dissemination in IoT using a cognitive UAV," *IEEE Trans. Cognit. Commun. Netw.*, vol. 5, no. 4, pp. 849–862, Dec. 2019.

[17] W. Khawaja, O. Ozdemir, and I. Guvenc, "UAV air-to-ground channel characterization for mmWave systems," in *Proc. IEEE 86th Veh. Technol. Conf. (VTC-Fall)*, Sep. 2017, pp. 1–5.

[18] S. Zhang, H. Zhang, Q. He, K. Bian, and L. Song, "Joint trajectory and power optimization for UAV relay networks," *IEEE Commun. Lett.*, vol. 22, no. 1, pp. 161–164, Jan. 2018.

[19] Z. M. Fadlullah, D. Takaishi, H. Nishiyama, N. Kato, and R. Miura, "A dynamic trajectory control algorithm for improving the communication throughput and delay in UAV-aided networks," *IEEE Netw.*, vol. 30, no. 1, pp. 100–105, Jan. 2016.

[20] Y. Zeng, X. Xu, and R. Zhang, "Trajectory design for completion time minimization in UAV-enabled multicasting," *IEEE Trans. Wireless Commun.*, vol. 17, no. 4, pp. 2233–2246, Apr. 2018.

[21] P. Yang, X. Cao, X. Xi, W. Du, Z. Xiao, and D. Wu, "Three-dimensional continuous movement control of drone cells for energy-efficient communication coverage," *IEEE Trans. Veh. Technol.*, vol. 68, no. 7, pp. 6535–6546, Jul. 2019.

[22] V. Saxena, J. Jalden, and H. Klessig, "Optimal UAV base station trajectories using flow-level models for reinforcement learning," *IEEE Trans. Cognit. Commun. Netw.*, vol. 5, no. 4, pp. 1101–1112, Dec. 2019.

[23] J. Lyu, Y. Zeng, and R. Zhang, "UAV-aided offloading for cellular hotspot," *IEEE Trans. Wireless Commun.*, vol. 17, no. 6, pp. 3988–4001, Jun. 2018.

[24] F. Cheng *et al.*, "UAV trajectory optimization for data offloading at the edge of multiple cells," *IEEE Trans. Veh. Technol.*, vol. 67, no. 7, pp. 6732–6736, Jul. 2018.

[25] Y. Zeng and R. Zhang, "Energy-efficient UAV communication with trajectory optimization," *IEEE Trans. Wireless Commun.*, vol. 16, no. 6, pp. 3747–3760, Jun. 2017.

[26] J. Zhang, Y. Wu, G. Min, F. Hao, and L. Cui, "Balancing energy consumption and reputation gain of UAV scheduling in edge computing," *IEEE Trans. Cognit. Commun. Netw.*, vol. 6, no. 4, pp. 1204–1217, Dec. 2020.

[27] L. Zhu, J. Zhang, Z. Xiao, X. Cao, D. O. Wu, and X.-G. Xia, "3-D beamforming for flexible coverage in millimeter-wave UAV communications," *IEEE Wireless Commun. Lett.*, vol. 8, no. 3, pp. 837–840, Jun. 2019.

[28] Z. Xiao, H. Dong, L. Bai, D. O. Wu, and X.-G. Xia, "Unmanned aerial vehicle base station (UAV-BS) deployment with millimeter-wave beamforming," *IEEE Internet Things J.*, vol. 7, no. 2, pp. 1336–1349, Feb. 2020.

[29] Z. Xiao, L. Zhu, and X.-G. Xia, "UAV communications with millimeter-wave beamforming: Potentials, scenarios, and challenges," *China Commun.*, vol. 17, no. 9, pp. 147–166, Sep. 2020.

[30] M. Alzenad, A. El-Keyi, and H. Yanikomeroglu, "3-D placement of an unmanned aerial vehicle base station for maximum coverage of users with different QoS requirements," *IEEE Wireless Commun. Lett.*, vol. 7, no. 1, pp. 38–41, Feb. 2018.

[31] R. I. B. Yaliniz, A. El-Keyi, and H. Yanikomeroglu, "Efficient 3-D placement of an aerial base station in next generation cellular networks," in *Proc. IEEE Int. Conf. Commun. (ICC)*, May 2016, pp. 1–5.

[32] Y. Chen, N. Li, C. Wang, W. Xie, and J. Xv, "A 3D placement of unmanned aerial vehicle base station based on multi-population genetic algorithm for maximizing users with different QoS requirements," in *Proc. IEEE 18th Int. Conf. Commun. Technol. (ICCT)*, Oct. 2018, pp. 967–972.

[33] M. Alzenad, A. El-Keyi, F. Lagum, and H. Yanikomeroglu, "3-D placement of an unmanned aerial vehicle base station (UAV-BS) for energy-efficient maximal coverage," *IEEE Wireless Commun. Lett.*, vol. 6, no. 4, pp. 434–437, Aug. 2017.

[34] M. Mozaffari, W. Saad, M. Bennis, and M. Debbah, "Efficient deployment of multiple unmanned aerial vehicles for optimal wireless coverage," *IEEE Commun. Lett.*, vol. 20, no. 8, pp. 1647–1650, Aug. 2016, doi: 10.1109/LCOMM.2016.2578312.

[35] M. Mozaffari, W. Saad, M. Bennis, and M. Debbah, "Drone small cells in the clouds: Design, deployment and performance analysis," in *Proc. IEEE Global Commun. Conf. (GLOBECOM)*, Dec. 2014, pp. 1–6.

[36] J. Lyu, Y. Zeng, R. Zhang, and T. J. Lim, "Placement optimization of UAV-mounted mobile base stations," *IEEE Commun. Lett.*, vol. 21, no. 3, pp. 604–607, Mar. 2017.

[37] I. Strumberger, N. Bacanin, S. Tomic, M. Beko, and M. Tuba, "Static drone placement by elephant herding optimization algorithm," in *Proc. 25th Telecommun. Forum (TELFOR)*, Nov. 2017, pp. 1–4.

[38] G.-G. Wang, S. Deb, and L. D. S. Coelho, "Elephant herding optimization," in *Proc. 3rd Int. Symp. Comput. Bus. Intell. (ISCBI)*, Dec. 2015, pp. 1–5.

[39] H. Zhao, H. Wang, W. Wu, and J. Wei, "Deployment algorithms for UAV airborne networks toward on-demand coverage," *IEEE J. Sel. Areas Commun.*, vol. 36, no. 9, pp. 2015–2031, Sep. 2018.

[40] C. H. Liu, Z. Chen, J. Tang, J. Xu, and C. Piao, "Energy-efficient UAV control for effective and fair communication coverage: A deep reinforcement learning approach," *IEEE J. Sel. Areas Commun.*, vol. 36, no. 9, pp. 2059–2070, Sep. 2018.

[41] J. Qin, Z. Wei, C. Qiu, and Z. Feng, "Edge-prior placement algorithm for UAV-mounted base stations," in *Proc. IEEE Wireless Commun. Netw. Conf. (WCNC)*, Apr. 2019, pp. 1–6.

[42] H. Wang, H. Zhao, W. Wu, J. Xiong, D. Ma, and J. Wei, "Deployment algorithms of flying base stations: 5G and beyond with UAVs," *IEEE Internet Things J.*, vol. 6, no. 6, pp. 10009–10027, Dec. 2019.

[43] G. Yang, Y.-C. Liang, R. Zhang, and Y. Pei, "Modulation in the air: Backscatter communication over ambient OFDM carrier," *IEEE Trans. Commun.*, vol. 66, no. 3, pp. 1219–1233, Mar. 2018.

[44] G. Yang, Q. Zhang, and Y.-C. Liang, "Cooperative ambient backscatter communications for green Internet-of-Things," *IEEE Internet Things J.*, vol. 5, no. 2, pp. 1116–1130, Apr. 2018.

[45] X. Kang, Y.-C. Liang, and J. Yang, "Riding on the primary: A new spectrum sharing paradigm for wireless-powered IoT devices," *IEEE Trans. Wireless Commun.*, vol. 17, no. 9, pp. 6335–6347, Sep. 2018.

[46] Y. Zeng, Q. Wu, and R. Zhang, "Accessing from the sky: A tutorial on UAV communications for 5G and beyond," *Proc. IEEE*, vol. 107, no. 12, pp. 2327–2375, Dec. 2019.

[47] J. T. Linderoth and M. W. P. Savelsbergh, "A computational study of search strategies for mixed integer programming," *Informs J. Comput.*, vol. 11, no. 2, pp. 173–187, May 1999.

[48] J. Tian, Y. Pei, Y.-D. Huang, and Y.-C. Liang, "Modulation-constrained clustering approach to blind modulation classification for MIMO systems," *IEEE Trans. Cognit. Commun. Netw.*, vol. 4, no. 4, pp. 894–907, Dec. 2018.

[49] Q. Zhang, H. Guo, Y.-C. Liang, and X. Yuan, "Constellation learning-based signal detection for ambient backscatter communication systems," *IEEE J. Sel. Areas Commun.*, vol. 37, no. 2, pp. 452–463, Feb. 2019.

[50] L. Zhu, J. Zhang, Z. Xiao, X. Cao, D. O. Wu, and X.-G. Xia, "Millimeter-wave NOMA with user grouping, power allocation and hybrid beamforming," *IEEE Trans. Wireless Commun.*, vol. 18, no. 11, pp. 5065–5079, Nov. 2019.

[51] L. Zhu, J. Zhang, Z. Xiao, X. Cao, and D. O. Wu, "Optimal user pairing for downlink non-orthogonal multiple access (NOMA)," *IEEE Wireless Commun. Lett.*, vol. 8, no. 2, pp. 328–331, Apr. 2019.

[52] D. Karaboga, "An idea based on honey bee swarm for numerical optimization," Tech. Rep. tr06, Erciyes Univ., Kayseri, Turkey, Jan. 2005.

[53] S. Boyd and L. Vandenberghe, *Convex Optimization*. Cambridge, U.K.: Cambridge Univ. Press, 2004.

[54] Y. Liu, K. Liu, J. Han, L. Zhu, Z. Xiao, and X.-G. Xia, "Resource allocation and 3D placement for UAV-enabled energy-efficient IoT communications," *IEEE Internet Things J.*, early access, Jun. 19, 2020, doi: 10.1109/JIOT.2020.3003717.

[55] E. Kalantari, H. Yanikomeroglu, and A. Yongacoglu, "On the number and 3D placement of drone base stations in wireless cellular networks," in *Proc. IEEE 84th Veh. Technol. Conf. (VTC-Fall)*, Sep. 2016, pp. 1–6.

[56] M. Mozaffari, W. Saad, M. Bennis, Y.-H. Nam, and M. Debbah, "A tutorial on UAVs for wireless networks: Applications, challenges, and open problems," *IEEE Commun. Surveys Tuts.*, vol. 21, no. 3, pp. 2334–2360, 3rd Quart., 2019.

Chen Zhang received the B.E. degree from the Department of Electronics and Information Engineering, Beihang University, Beijing, China, in 2018, where he is currently pursuing the Ph.D. degree. His research interests include UAV communications and spectrum sensing.

Leyi Zhang received the B.E. degree with the Department of Electronics and Information Engineering, Beihang University, Beijing, China, in 2020, where she is currently pursuing the M.S. degree with the Department of Electronic and Information Engineering. Her research interests include UAV communications and spectrum sensing.

Lipeng Zhu (Graduate Student Member, IEEE) received the B.S. degree from the Department of Mathematics and System Sciences, Beihang University, in 2017, where he is currently pursuing the Ph.D. degree with the Department of Electronic and Information Engineering. His research interest is millimeter-wave communications, non-orthogonal multiple access, and UAV communications.

Tao Zhang (Member, IEEE) was born in 1973. He received the B.S.E.E. degree from the Huazhong University of Science and Technology, Wuhan, China, in 1995, and the Ph.D. degree from Beihang University, Beijing, China, in 2006. He is currently a Professor of the School of Electronics and Information Engineering, Beihang University. His research interests include mobile communication and satellite network communication.

Zhenyu Xiao (Senior Member, IEEE) received the B.E. degree from the Department of Electronics and Information Engineering, Huazhong University of Science and Technology, Wuhan, China, in 2006, and the Ph.D. degree from the Department of Electronic Engineering, Tsinghua University, Beijing, China, in 2011. From 2011 to 2013, he held a post-doctoral position with the Department of Electronic Engineering, Tsinghua University. He was with the School of Electronic and Information Engineering, Beihang University, Beijing, as a Lecturer, from 2013 to 2016, and an Associate Professor from 2016 to 2020, where he is currently a Full Professor. He has visited the University of Delaware from 2012 to 2013 and the Imperial College London from 2015 to 2016.

He has authored or coauthored over 70 articles, including the IEEE JSAC, IEEE TWC, IEEE TSP, IEEE TVT, IEEE COMML, IEEE WCL, and IET COMM. He is an active researcher with broad interests on millimeter wave communications and UAV/satellite communications and networking. He has been a TPC member of the IEEE GLOBECOM, IEEE WCSP, IEEE ICC, and IEEE ICCC. He has received 2017 Best Reviewer Award of the IEEE TWC, the 2019 Exemplary Reviewer Award of the IEEE WCL, and the 4th China Publishing Government Award. He has received the Second Prize of National Technological Invention, the First Prize of Technical Invention of China Society of Aeronautics and Astronautics, and the Second Prize of Natural Science of China Electronics Society. He is currently an Associate Editor for IEEE TRANSACTIONS ON COGNITIVE COMMUNICATIONS AND NETWORKING, *China Communications*, *IET Communications*, the *KSII transactions on Internet and Information Systems*, and *Frontiers in Communications and Networks*. He has also been a leading Guest Editor of a Special Issue *Space-Air-Ground Integrated Network with Native Intelligence (NI-SAGIN): Concept, Architecture, Technology, and Radio* of *China Communications*.

Xiang-Gen Xia (Fellow, IEEE) received the B.S. degree in mathematics from Nanjing Normal University, Nanjing, China, and the M.S. degree in mathematics from Nankai University, Tianjin, China, and the Ph.D. degree in electrical engineering from the University of Southern California, Los Angeles, in 1983, 1986, and 1992, respectively.

He was a Senior/Research Staff Member with Hughes Research Laboratories, Malibu, CA, USA, from 1995 to 1996. In 1996, he joined the Department of Electrical and Computer Engineering, University of Delaware, Newark, Delaware, where he is currently the Charles Black Evans Professor. He has authored the book *Modulated Coding for Intersymbol Interference Channels* (New York, Marcel Dekker, 2000). His current research interests include space–time coding, MIMO and OFDM systems, digital signal processing, and SAR and ISAR imaging.

Dr. Xia received the National Science Foundation Faculty Early Career Development (CAREER) Program Award in 1997, the Office of Naval Research Young Investigator Award in 1998, and the Outstanding Overseas Young Investigator Award from the National Nature Science Foundation of China in 2001. He received the 2019 Information Theory Outstanding Overseas Chinese Scientist Award, The Information Theory Society of Chinese Institute of Electronics. He was the General Co-Chair of the ICASSP 2005 in Philadelphia and the Technical Program Chair of the Signal Processing Symposium Globecom 2007 in Washington, DC, USA. He has served as an Associate Editor for numerous international journals, including IEEE WIRELESS COMMUNICATIONS LETTERS, IEEE TRANSACTIONS ON SIGNAL PROCESSING, IEEE TRANSACTIONS ON WIRELESS COMMUNICATIONS, IEEE TRANSACTIONS ON MOBILE COMPUTING, and IEEE TRANSACTIONS ON VEHICULAR TECHNOLOGY.